Phospholipase C-linked receptors regulate the ATP-sensitive potassium channel by means of phosphatidylinositol 4,5-bisphosphate metabolism

Lai-Hua Xie*, Minoru Horie†, and Makoto Takano*‡

Departments of *Physiology and Biophysics, and †Cardiovascular Medicine, Graduate School of Medicine, Kyoto University, Kyoto 606-8501, Japan

Edited by Lily Yeh Jan, University of California, San Francisco, CA, and approved October 15, 1999 (received for review May 17, 1999)

In the COS7 cells transfected with cDNAs of the Kir6.2, SUR2A, and M_1 muscarinic receptors, we activated the ATP-sensitive potassium (K_{ATP}) channel with a K^+ channel opener and recorded the whole-cell K_{ATP} current. The K_{ATP} current was reversibly inhibited by the stimulation of the M_1 receptor, which is linked to phospholipase C (PLC) by the G_q protein. The receptor-mediated inhibition was observed even when protein kinase C (PKC) was inhibited by H-7 or by chelating intracellular Ca^{2+} with 10 mM 1,2-bis(2-aminophenoxy)ethane-*N*,*N*,*N*′,*N*′-tetraacetate (BAPTA) included in the pipette solution. However, the receptor-mediated inhibition was blocked by U-73122, a PLC inhibitor. M_1-receptor stimulation failed to inhibit the K_{ATP} current activated by the injection of exogenous phosphatidylinositol 4,5-bisphosphate (PIP_2) through the whole-cell patch pipette. The receptor-mediated inhibition became irreversible when the replenishment of PIP_2 was blocked by wortmannin (an inhibitor of phosphatidylinositol kinases), or by including adenosine 5′-[β,γ–imido]triphosphate (AMPPNP, a nonhydrolyzable ATP analogue) in the pipette solution. In inside-out patch experiments, the ATP sensitivity of the K_{ATP} channel was significantly higher when the M_1 receptor in the patch membrane was stimulated by acetylcholine. The stimulatory effect of pinacidil was also attenuated under this condition. We postulate that stimulation of PLC-linked receptors inhibited the K_{ATP} channel by increasing the ATP sensitivity, not through PKC activation, but most probably through changing PIP_2 levels.

The ATP-sensitive potassium (K_{ATP}) channels play a key role in the coupling between cellular metabolism and electrical activity in a wide range of tissues. Although the primary characteristic of the K_{ATP} channel is the inhibition by intracellular ATP, various cytosolic substances, such as divalent cations, protons, anions, and nucleoside diphosphates, are known as modulators of the K_{ATP} channel (1–4).

In addition to the cytosolic factors listed above, a component of membrane lipid bilayer also modulates the K_{ATP} channel; phosphatidylinositol (PI)-4,5-bisphosphate (PIP_2) is known to increase the open probability and decrease the ATP sensitivity of the cardiac and reconstituted K_{ATP} channel (5–8). Membrane PIP_2 content increases when PI and PI 4-monophosphate (PIP) are consecutively phosphorylated by PI 4-kinase and PIP 5-kinase (9). On the other hand, PIP_2 content should decrease when PIP_2 is dephosphorylated by inositolpolyphosphate phosphatase (10) or hydrolyzed by phospholipase C (PLC). In fact, it has been reported that the receptor-mediated activation of PLC decreased PIP_2 content in the plasma membrane of Chinese hamster ovary (CHO) cells and human neuroblastoma cells (11, 12).

PLC-linked receptors are distributed in many tissues, including cardiac myocytes and pancreatic β-cells, where K_{ATP} channels are also present. This raises the question of whether PLC-linked receptors might modulate the K_{ATP} channel by changing PIP_2 levels (8) and ultimately affect the coupling between intracellular metabolism and electrical activity. Therefore, we examined the effects of receptor-mediated activation of PLC on the cloned K_{ATP} channel (Kir6.2 and SUR2A) (13–15) expressed in COS7 cells. We demonstrate that the stimulation of the PLC-linked receptor modulates the K_{ATP} channel without the activation of protein kinase C (PKC), most probably through the depletion of the PIP_2 pool in the plasma membrane.

Methods

Molecular Biology. cDNAs of Kir6.2, SUR2A, and green fluorescent protein [GFP(S65A)] were subcloned into the pCI vector (Promega). The M_1 muscarinic receptor cDNA was subcloned into an expression vector carrying the simian virus 40 promoter. Mixtures of the following amounts of vectors (μg per dish) were cotransfected into COS7 cells with Lipofectamine reagent and Opti-MEM (GIBCO/BRL): 0.8 Kir6.2 + 0.8 SUR2A + 0.4 GFP + 1.6 receptor. COS7 cells were cultured in DMEM supplemented with 10% (vol/vol) FCS.

Electrophysiology. After the transfection (24–48 hr), the whole-cell and inside-out patch experiments were performed in GFP-positive cells with an Axopatch 200B amplifier (Axon Instruments, Foster City, CA). The current and voltage signals were stored on a DAT tape recorder (TEAC, Tokyo, Japan) as well as an on-line computer (PC-98; NEC, Tokyo, Japan) through an analog–digital converter (ADX98E; Canopus, Osaka, Japan). The current signals were also played back and digitized with a Digipack 1200A interface (Axon Instruments). Data analysis was carried out by using in-house-made programs and commercial software (pClamp 6 & 7; Axon Instruments).

Solutions. The physiological saline contained (in mM): 140 NaCl, 5.4 KCl, 1 Na_2HPO_4, 1.8 $CaCl_2$, 0.5 $MgCl_2$, 5 glucose, and 5 Hepes (pH 7.4 with NaOH). The high K^+ whole-cell pipette solution contained (in mM): 110 aspartic acid, 10 NaCl, 1 $MgCl_2$, 4 ATP, 0.1 GTP, 10 1,2-bis(2-aminophenoxy)ethane-*N*,*N*,*N*′,*N*′-tetraacetate (BAPTA), 5 Hepes (pH 7.4 with KOH). In some experiments, ATP was replaced with the same amount of adenosine 5′-[β,γ–imido]triphosphate (AMPPNP), or 0.1 mM GTP was replaced with 1 mM guanosine 5′-[β-thio]triphosphate (GDPβS). The inside-out patch pipette solution contained (in mM): 140 KCl, 1 $CaCl_2$, 1 $MgCl_2$, and 5 Hepes (pH 7.4 with KOH). The control internal solution for the inside-out patch experiments contained: 140 KCl, 2 $MgCl_2$, 2 EGTA, and 5 Hepes (pH 7.2 with KOH). Li_4AMPPNP, pinacidil, acetylcholine (ACh), and H-7 were purchased from Sigma. PIP_2 (Calbiochem)

This paper was submitted directly (Track II) to the PNAS office.

Abbreviations: K_{ATP}, ATP-sensitive potassium; PLC, phospholipase C; PI, phosphatidylinositol; PIP_2, PI 4,5-bisphosphate; PIP, PI 4-monophosphate; GFP, green fluorescent protein; CHO, Chinese hamster ovary; PKC, protein kinase C; ACh, acetylcholine; WMN, wortmannin; DAG, diacylglycerol; *I–V*, current–voltage; BAPTA, 1,2-bis(2-aminophenoxy)ethane-*N*,*N*,*N*′,*N*′-tetraacetate; AMPPNP, adenosine 5′-[β,γ–imido]triphosphate; GDPβS, guanosine 5′-[β-thio]triphosphate.

‡To whom reprint requests should be addressed. E-mail: takanom@card.med.kyoto-u.ac.jp.

The publication costs of this article were defrayed in part by page charge payment. This article must therefore be hereby marked "*advertisement*" in accordance with 18 U.S.C. §1734 solely to indicate this fact.

was dissolved in the control internal solution by sonication for 30 min on ice. U-73122, (Wako Pure Chemicals, Osaka) wortmannin (WMN; Wako), LY 294002 (Tocris Neuramin, Bristol, U.K.), and diacylglycerol (DAG; Serdary Research Laboratories, Englewood Cliffs, NJ) were first dissolved in DMSO as a stock solution, and then used at the final concentration in the solution. The test solutions were applied either by bath perfusion or by a Y-tube apparatus (16). The whole-cell experiments were conducted at 37°C, and the inside-out patch experiments were conducted at 22–25°C.

Data Analysis. The whole-cell current–voltage (*I–V*) relationship was measured with ramp pulses (120 mV/s) applied every 6 s from the holding potential of −60 mV; initial positive slope from −60 mV to 0 mV was followed by a negative slope to −120 mV, and the *I–V* relationship was determined from the negative limb of the ramp pulse. The membrane potentials were corrected for the liquid-junction potential (≈10 mV) between the pipette solution and the physiological saline. In the inside-out patch experiments, the amplitude of mean patch current (MPC; the integral of open-channel current divided by the time for integration) was measured for 5–10 s, before (MPC_{CTR}) and after (MPC_{ATP}) the application of ATP. The magnitude of inhibition was calculated as: $(MPC_{CTR} - MPC_{ATP})/MPC_{CTR}$. The data points are expressed as mean ± SEM. The Hill equation fitted to the data points is described in the legend of Fig. 1. The statistical analyses were performed using the Student's unpaired *t* test, with $P < 0.05$ being considered significant. The mean value was obtained from at least five observations in each experiment.

Results

Stimulation of the PLC-Linked Receptor Inhibited the Whole-Cell K_{ATP} Current. COS7 cells are known to possess the PI signal transduction pathway (17). We have confirmed that the application of ACh produced Ca^{2+} mobilization in the COS7 cells transfected with the M_1 muscarinic receptor by measuring fura-2 fluorescence (data not shown). In the experiment shown in Fig. 1, cloned K_{ATP} channels (Kir6.2 + SUR2A) were coexpressed with (Fig. 1 *A* and *C*) or without (Fig. 1*B*) M_1 receptors. It is well known that intracellular Ca^{2+} promotes the rundown of the K_{ATP} channel (1). To exclude the effects of intracellular Ca^{2+}, we carried out whole-cell patch experiments using the pipette solution containing 10 mM BAPTA. Thereby, intracellular Ca^{2+} concentration of COS7 cells was clamped to $\approx 10^{-10}$ M. Even under this condition, ACh reversibly inhibited the K_{ATP} current, which was activated by 100 μM pinacidil (18), in the COS7 cells expressing the M_1 receptor (Fig. 1*A*), whereas ACh was without the inhibitory effect in the COS7 cell that was not transfected with the M_1 receptor (Fig. 1*B*). When a low-ATP pipette solution containing 10 μM ATP was used, the K_{ATP} current occurred spontaneously after the formation of whole-cell configuration. Under this condition, ACh also inhibited the K_{ATP} current in a reversible manner (Fig. 1*C*).

In both experiments shown in Fig. 1 *A* and *C*, the onset of receptor-mediated inhibition of the K_{ATP} current was very slow; it took ≈1 min to reach the steady state. Recovery from the receptor-mediated inhibition also proceeded in a slow time course (≈5 min). The recovery was sometimes incomplete, particularly when the K_{ATP} current was activated by a low ATP pipette solution. Time courses of the receptor-mediated inhibition and recovery of the K_{ATP} current closely resembled those of receptor-mediated depletion and replenishment of PIP_2 reported in CHO cells and human neuroblastoma cells (11, 12).

The dose-inhibition relationship for ACh was examined in Fig. 1*A*. Because the recovery from the receptor-mediated inhibition was sometimes incomplete, various concentrations of ACh were applied in a cumulative manner; the amplitude of the current deflection became smaller as ACh concentration increased. The

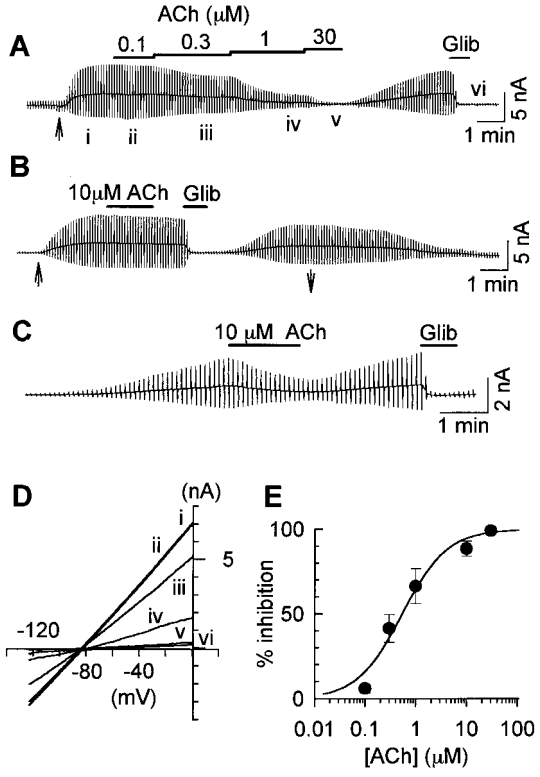

Fig. 1. M_1 receptor-mediated inhibition of the K_{ATP} current. Chart recordings of whole-cell current recorded in the COS7 cell cotransfected with Kir6.2, SUR2A, and M_1 receptor cDNA. The current deflections are the results of ramp pulses. (*A*) The perfusion of 100 μM pinacidil started at the time indicated by the arrow (↑) under the current trace. The applications of ACh and 10 μM glibenclamide are indicated by the horizontal lines above the trace. (*B*) The whole-cell K_{ATP} current recorded in the COS7 cell that was not cotransfected with the M_1 receptor. The perfusion of 100 μM pinacidil started at the time indicated by ↑ and finished at ↓ under the trace. (*C*) Spontaneous activation of the K_{ATP} current after the formation of the whole-cell patch using the pipette solution containing 10 μM ATP. (*D*) *I–V* relationships obtained at the times indicated by i–vi in *A*. The reversal potential was ≈−85 mV. (*E*) Concentration-inhibition relationship for ACh. The percent inhibition was plotted against ACh concentration. The following Hill equation is fitted to each data point: % inhibition = $100/\{1 + (IC_{50}/[ACh])^{n}H\}$, where IC_{50} is the concentration for the half-maximal inhibition, and n_H is the Hill coefficient. $IC_{50} = 0.54 \pm 0.12$ μM, and $n_H = 0.98 \pm 0.22$ ($n = 6$). The line was drawn with these values.

I–V relationships measured at the times i–vi are shown in Fig. 1*D*. All of the *I–V* curves showed weak inward rectification and intersected each other at the potential close to the equilibrium potential for K^+. The amplitude of the K_{ATP} current was measured at 0 mV before and during the application of ACh. The magnitude of the receptor-mediated inhibition (% inhibition) was determined as follows: % inhibition = $(I_{CTR} - I_{ACh})/I_{CTR}$, where I_{CTR} is the amplitude of the glibenclamide-sensitive current (i–vi), and I_{ACh} is the amplitude during ACh application (e.g., for 1 μM ACh, iv–vi). The concentration-inhibition relationships are shown in Fig. 1*E*. The concentration producing the half-maximal inhibition (IC_{50}) was 0.54 ± 0.12 μM, and the Hill coefficient (n_H) was 0.98 ± 0.22.

Under the same experimental conditions, stimulation of PLC by endothelin or by the α1-adrenergic agonist inhibited the K_{ATP} current in rat ventricular myocytes, but not in guinea-pig and rabbit myocytes (Xie *et al.*, unpublished observation). It has been reported that in rat ventricular myocytes, stimulation of endothelin receptor antagonizes the production of cAMP by means of the pertussis toxin (PTX)-sensitive mechanism, and simulta-

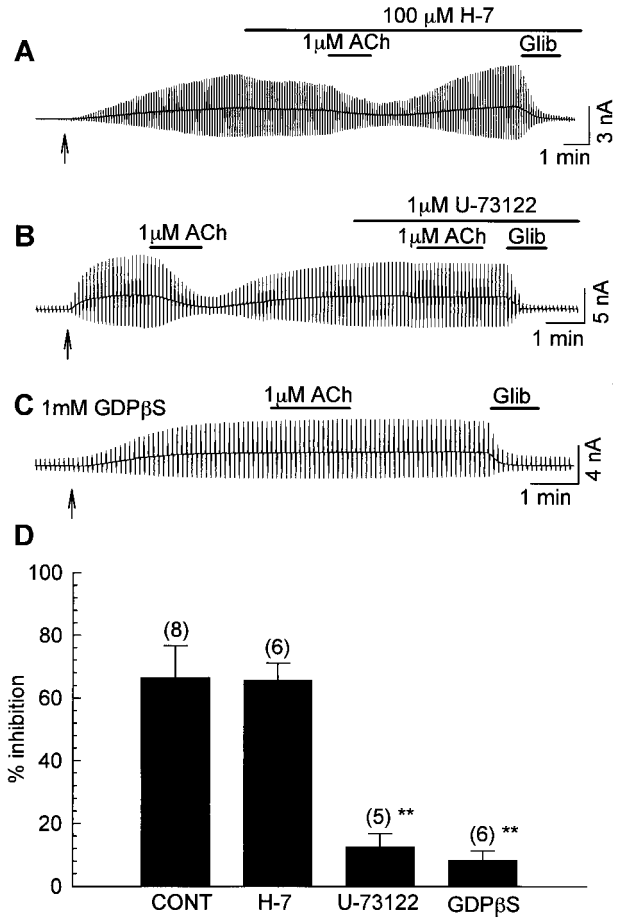

Fig. 2. Effects of H-7, U-73122, and GDPβS on M_1 receptor-mediated inhibition of the K_{ATP} current. The COS7 cells were cotransfected with cDNAs of Kir6.2, SUR2A, and the M_1 receptor. The K_{ATP} current was activated by the perfusion of 100 μM pinacidil (started at $\uparrow$). (*A*) The effect of H-7 on M_1 receptor-mediated inhibition. The applications of 1 μM ACh, 100 μM H-7, and 10 μM glibenclamide are indicated by the bars above the recording. (*B*) The effect of 1 μM U-73122. (*C*) A COS7 cell was dialyzed with the pipette solution containing 1 mM GDPβS. (*D*) Summary of the magnitudes of 1 μM ACh-induced maximal inhibition of the K_{ATP} current in control, H-7-, U-73122-, and GDPβS-treated cells. The numerals in parentheses indicate numbers of experiments. **, $P < 0.01$ vs. control.

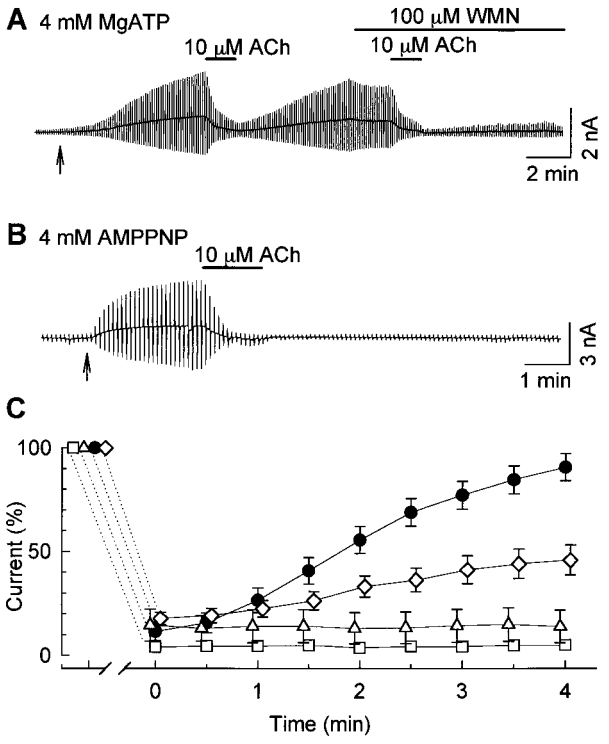

Fig. 3. The time course for receptor-mediated inhibition and the blocking of PIP_2 replenishment. Whole-cell K_{ATP} currents were activated by 100 μM pinacidil, which started at the times indicated by the arrows. (*A*) The inhibitory effects of 10 μM ACh before and after the application of 100 μM WMN. The applications of ACh and WMN are indicated by the bars above the recording. (*B*) The effect of intracellular dialysis with the pipette solution containing 4 mM AMPPNP. (*C*) The summary of recovery time courses after the washout of ACh. ●, Control; ◇, 10 μM WMN; □, 100 μM WMN; △, 4 mM AMPPNP in the pipette. At 4 min, the magnitudes of currents were 90.6 ± 6.6%, 46.0 ± 7.3%, 5.0 ± 0.2%, and 13.9 ± 7.9% of the control, respectively.

neously promotes PI turnover by the PTX-insensitive pathway (19). The latter signal transduction pathway might not be significant in guinea pig and rabbit myocytes.

PLC, but Not PKC, Was Involved in the Inhibition. In all of the experiments in the present study, the pipette solutions contained 10 mM BAPTA, which should chelate intracellular Ca^{2+} completely. Therefore, it seems unlikely that Ca^{2+}-dependent PKC was activated during the receptor stimulation. To elucidate the mechanisms for the receptor-mediated inhibition, we blocked each step of the signal transduction pathway. In Fig. 2*A*, the K_{ATP} current was activated by pinacidil. The following application of 100 μM H-7, a blocker of PKC, slightly inhibited the current. Under this condition, 1 μM ACh successfully inhibited the K_{ATP} current. The magnitude of the inhibition was not significantly different from the control experiments (65.5 ± 5.5%, $P > 0.05$ vs. control: 66.4 ± 10.1%; Fig. 2*D*), suggesting that the activation of PKC was not involved in the receptor-mediated inhibition of the K_{ATP} current.

However, when PLC was blocked by 1 μM U-73122, the receptor-mediated inhibition was significantly attenuated. In the experiment shown in Fig. 2*B*, we first inhibited the K_{ATP} current by the application of 1 μM ACh. After the K_{ATP} current was recovered to the control level, 1 μM ACh was applied in the presence of U-73122. Clearly, 1 μM U-73122 abolished ACh-induced inhibition. As summarized in Fig. 2*D*, the magnitude of inhibition was 12.4 ± 4.4% under this condition ($P < 0.01$). Blocking GTP-binding protein also attenuated the receptor-mediated inhibition. In the experiment shown in Fig. 2*C*, the pipette solution contained 1 mM GDPβS (a nonspecific blocker of GTP-binding proteins) instead of 0.1 mM GTP. Under this condition, the inhibitory effect of 1 μM ACh was significantly attenuated (8.1 ± 3.1%, $P < 0.01$). Based on the above findings, we postulated that the receptor-mediated inhibition was the result of the activation of PLC, but not the activation of PKC. The most plausible mechanism might be the depletion of PIP_2.

The Blockade of PIP_2 Synthesis Obstructed the Recovery from the Receptor-Mediated Inhibition. In CHO cells and human neuroblastoma cells, the receptor-mediated activation of PLC produced a depletion of PIP_2 in the plasma membrane. WMN (an inhibitor of PI 3-kinase and PI 4-kinase) inhibited the replenishment of PIP_2 after the depletion (12). Therefore, we examined whether the inhibition of PIP_2 replenishment by WMN was reflected in the recovery of the K_{ATP} current from the receptor-mediated inhibition. In Fig. 3*A*, we first applied 10 μM ACh to inhibit the K_{ATP} current and confirmed the recovery after washout of ACh. As summarized in Fig. 3*C* (●), the K_{ATP} current

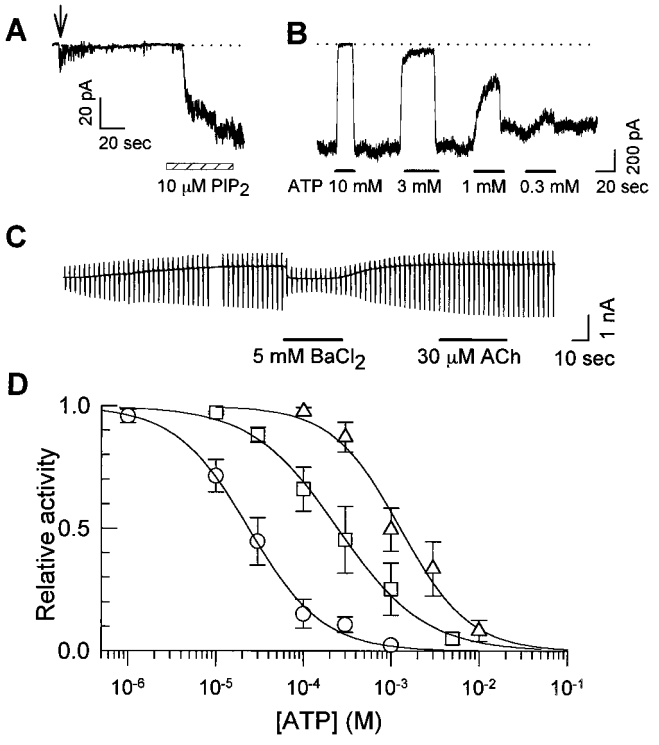

Fig. 4. The effect of exogenous PIP_2 on the ATP sensitivity. (*A*) The time course of PIP_2 activation in an inside-out patch experiment. The patch was excised at the time indicated by the arrow. PIP_2 application is indicated by the hatched bar. (*B*) The inhibitory effect of ATP on K_{ATP} channels activated by PIP_2. PIP_2 (10 μM) was applied for 3 min before examining ATP sensitivity. The current traces in *A* and *B* were recorded in different patches. (*C*) The whole-cell K_{ATP} current activated by the pipette solution containing 100 μM PIP_2. After the application of positive pressure [$\approx$10 cmH_2O (1 cm H_2O = 88 Pa)], the K_{ATP} current started to occur. The holding potential was -20 mV. The ramp pulse was applied from -140 mV to 0 mV. $BaCl_2$ (5 mM) was applied to examine the reversal potential (≈ -85 mV). (*D*) Dose-inhibition curves for ATP. ○, Control; □, 40 s after the application of 10 μM PIP_2. △, 3 min after 10 μM PIP_2 application. The Hill equation fitted to data points is indicated in the legend of Fig. 5. IC_{50} values are indicated in the text.

was recovered to 90.8 ± 6.6% of the preceding level 4 min after the washout of ACh. In the presence of 100 μM WMN, the K_{ATP} current was no longer recovered after the washout of ACh (Fig. 3*A*). The amplitude of the K_{ATP} current measured at the end of the experiment was 5.0 ± 0.2% of the preceding level (□ in Fig. 3*C*, $P < 0.01$ vs. control). When we applied 10 μM WMN, the receptor-mediated inhibition was partially reversible (◇ in Fig. 3*C*, 46.0 ± 7.3%, $P < 0.01$). These results are in agreement with those obtained in our previous inside-out experiments on the MgATP-dependent recovery of the channel (20).

We next tried to block the replenishment of PIP_2 by replacing ATP with a nonhydrolyzable analogue, AMPPNP. In the experiment shown in Fig. 3 *B* and *C* (△) the pipette solution contained 4 mM AMPPNP instead of ATP. Because AMPPNP and ATP equally inhibit the K_{ATP} channel, no potassium current was activated after the formation of the whole-cell patch. The K_{ATP} current was then activated by 100 μM pinacidil. The following application of 10 μM ACh produced an irreversible inhibition of the K_{ATP} current. AMPPNP is commercially available only as the lithium salt. Jenkinson *et al.* (11) reported that Li^+ disrupts the supply of PIP_2 in CHO cells during the stimulation of PLC with a slow time course; the PIP_2 level became significantly lower 10–30 min after the stimulation of PLC (Fig. 4). However, the recovery of the K_{ATP} current was 86.6 ± 9.1% ($n = 6$, $P > 0.05$ vs. control) 4 min after the washout of ACh, when the pipette solution contained 4 mM ATP and 16 mM LiCl (data not shown). Li^+ may not inhibit the replenishment of PIP_2 during a short period of agonist application. Therefore, we presumed that the inhibition of the recovery of the K_{ATP} current was not because of Li, but because of AMPPNP itself.

The Stimulation of the PLC-Linked Receptor Shifted the ATP Sensitivity. In the previous section, we demonstrated that the stimulation of the M_1 receptor inhibited the pinacidil-induced K_{ATP} current without PKC activation. However, the mechanism beyond this point remains unclear. This mechanism might be explained in two ways. First, stimulation of the M_1 receptor may change the intracellular ATP concentration. Second, M_1 receptor stimulation may modulate the properties of the K_{ATP} channel. It has been reported that exogenous application of PIP_2 promoted the opening of the K_{ATP} channel and decreased the ATP sensitivity (7, 8). Therefore, when the stimulation of the M_1 receptor depletes the PIP_2 pool of the plasma membrane, it may produce the opposite effect on the K_{ATP} channel. We first confirmed that 10 μM PIP_2 markedly decreased the ATP sensitivity in the inside-out patch experiments. PIP_2 restored K_{ATP}-channel activity in a slow time course (Fig. 4*A*). In a different patch, ATP sensitivity was markedly decreased 3 min after PIP_2 application; 10 mM ATP was required to inhibit the K_{ATP} channel completely (Fig. 4*B*). Fig. 4*D* summarizes the dose-inhibition relationship; ATP concentration for the half-maximal inhibition (IC_{50}) was 23.4 ± 5.9 μM in control (○; also see Fig. 5 *A* and *B*). Forty seconds after the application of PIP_2, IC_{50} was 246.8 ± 18.1 μM (□, $P < 0.01$ vs. control). Prolonged application (3 min) produced a larger change in IC_{50} (△; 1276.5 ± 224.2 μM, $P < 0.01$).

Baukrowitz *et al.* (8) reported that injection of PIP_2 into *Xenopus* oocytes expressing Kir6.2 + SUR2A promoted a persistent activation of the K_{ATP} current. However, in the whole-cell patch experiments, we failed to activate the K_{ATP} current with the pipette solutions containing 100, 200, and 500 μM PIP_2. This was presumably because micellar PIP_2 solution could not passively diffuse into the cells. Therefore, we tried to inject the pipette solution containing 100 μM PIP_2 by applying positive pressure ($\approx$10 cmH_2O) to the patch pipette. In most cases, we lost the whole-cell patch by this manipulation. In 3 of 24 experiments, we could activate the K_{ATP} current (Fig. 4*C*). Under this condition, M_1-receptor stimulation failed to inhibit the K_{ATP} current.

We next stimulated M_1 receptors by including 30 μM ACh in the pipette solution and measured the ATP sensitivity. As shown in Fig. 5*A Upper*, 1 μM ATP did not inhibit the K_{ATP} channel under control conditions. In contrast, 1 μM ATP produced a sizable inhibition when the pipette solution contained 30 μM ACh (Fig. 5*A*, *Lower*). Fig. 5*B* summarizes the dose-inhibition relationship. IC_{50} was 23.4 ± 5.9 μM under control condition (○). In the presence of 30 μM ACh, ATP sensitivity was significantly higher (□; IC_{50} = 2.6 ± 0.4 μM, $P < 0.01$).

In the previous whole-cell experiments, the stimulation of the PLC-linked receptor inhibited the pinacidil-induced K_{ATP} current. Therefore, PLC activation may also increase the ATP sensitivity in the presence of pinacidil. In the experiments shown in Fig. 5 *C* and *D*, we applied 100 μM pinacidil to the cytoplasmic surface of the patch membrane and measured the ATP sensitivity in the comparable condition with the previous whole-cell experiments. Pinacidil altered IC_{50} from 23.4 ± 5.9 μM to 297.3 ± 56.5 μM (△; $P < 0.01$). When M_1 receptors were stimulated, the ATP sensitivity increased significantly in the presence of pinacidil (◇; IC_{50} = 7.9 ± 2.2 μM). Thus, it seemed likely that the receptor-mediated inhibition of the whole-cell K_{ATP} current was the result of the increase in ATP-sensitivity.

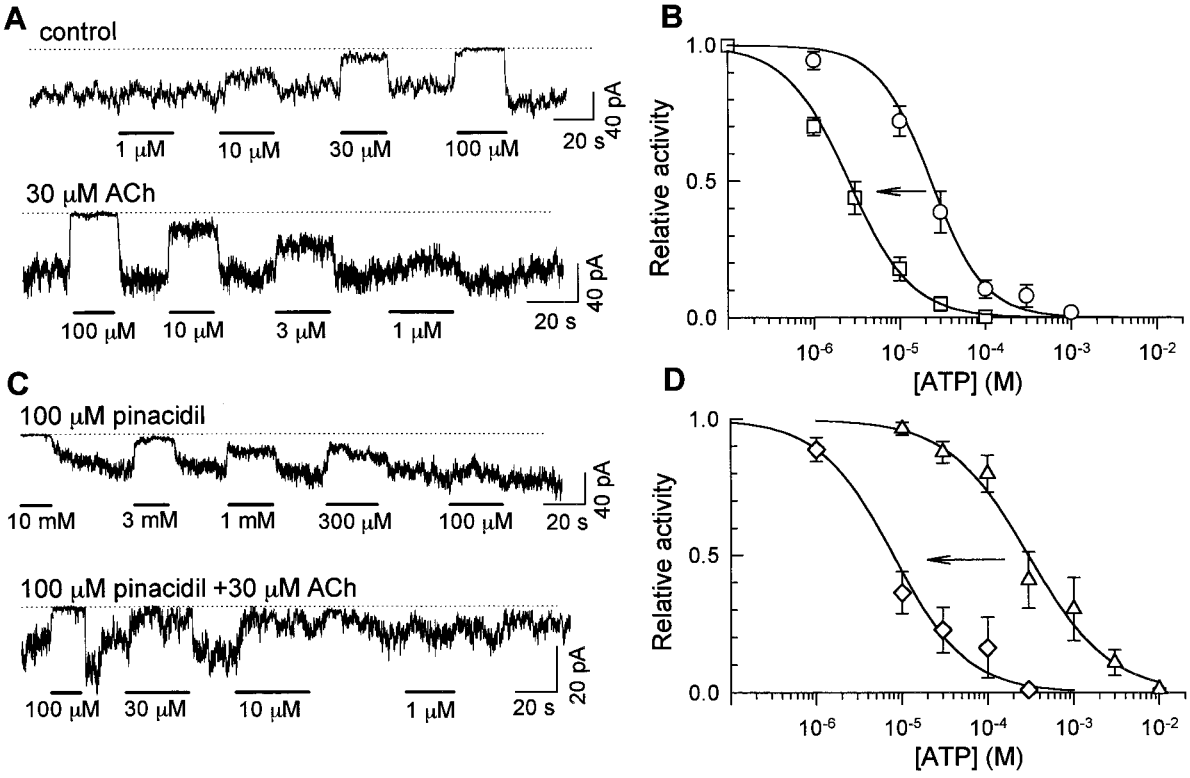

Fig. 5. Shift of the ATP sensitivity induced by M_1-receptor stimulation. (*A*) Effects of various concentrations of ATP in the absence (*Upper*) and presence (*Lower*) of 30 μM ACh in the pipette solution. The dotted lines indicate the closed channel levels. ATP concentrations are indicated below the current traces. (*B*) Dose-inhibition relationships for ATP. ○, Control. □, 30 μM ACh in the pipette solution. (*C*) Effects of various concentrations of ATP measured in the presence of 100 μM pinacidil. Pinacidil was applied to the intracellular side of the patch membrane. Otherwise, the experiment is the same as *A*. (*D*) Dose-inhibition curves for ATP measured in *C*. △, 100 μM pinacidil alone; ◇, 100 μM pinacidil plus 30 μM ACh in the pipette solution. (*B* and *D*) The Hill equation was fitted to each set data point: relative activity = $1/[1 + ([ATP]/IC_{50})^{n}H]$. The lines are drawn using the average values of IC_{50} and n_H. IC_{50} values are shown in the text; n_H values are not significantly different (0.9–1.4, $P > 0.05$), in both *B* and *D*.

Discussion

The present study has provided convincing evidence that the activation of the PLC-linked receptor inhibits the K_{ATP} channel (Kir6.2 + SUR2A), as previously suggested by Baukrowitz *et al.* (8). It has been reported that receptor-mediated activation of PLC reduces PIP_2 concentration by 84.9 ± 7.3% in human neuroblastoma cells (12). Although we have not carried out the biochemical measurements of PIP_2 concentration, it is likely that similar magnitude of PIP_2 depletion also occurs in COS7 cells. The stimulation of the PLC-linked receptor produces inositol trisphosphate (IP_3) and DAG. Exogenous application of IP_3 had no effect on K_{ATP}-channel activity (6, 7). In the present study, 10 μM DAG did not inhibit the K_{ATP} channel in inside-out patch experiments (data not shown), although 1,2-dioctanoyl-*sn*-glycerol (DOG), a membrane-permeant analogue of DAG, inhibited the K_{ATP} channel (6). It should be noted that other types of PI metabolites, such as IP_5 and IP_6, regulate the Ca^{2+} channel (20). Therefore, the involvement of such metabolites cannot be excluded in the present study. However, stimulation of the PLC-linked receptor did not inhibit the K_{ATP} current when exogenous PIP_2 was applied in the whole-cell patch experiment (Fig. 4*C*). This may partly support the idea that the mechanism of the receptor-mediated inhibition was the depletion of PIP_2, rather than the production of PI metabolites that may inhibit the K_{ATP} channel. This idea may also be supported by the finding that the receptor-mediated inhibition became irreversible when the replenishment of PIP_2 was blocked by WMN or AMPPNP.

So far, specific blockers for PI 4-kinase or PI 5-kinase have not been reported. WMN, an inhibitor of PI 3-kinase, blocks PI 4-kinase at a higher concentration. The concentration of WMN used in the present study was higher than those in the biochemical experiments used to block PI 4-kinase (12, 21, 22). At a low concentration (200 nM), WMN did not inhibit the recovery from the receptor-mediated inhibition (data not shown). Because WMN has a nonspecific effect on the enzymes other than PI kinases at higher concentration (23), unknown types of enzymes might be involved in the recovery from the receptor-mediated inhibition. Exogenous PIP_3 also activated the K_{ATP} channel (7), raising the question of whether WMN effect might be the result of the block of PI 3-, rather than PI 4-, kinase. However, the receptor-mediated inhibition was readily reversible in the presence of 10 μM LY294002, a specific PI 3-kinase blocker (ref. 24, and data not shown). Therefore, this finding supports the hypothesis that the WMN effect was the result of the block of PI 4-kinase. We previously reported that WMN inhibited the MgATP-dependent recovery of the K_{ATP} channel, most likely by blocking PIP_2 replenishment (25). LY294002 (10 μM) did not inhibit MgATP-dependent recovery (data not shown). WMN had similar dose-dependent effects on MgATP-dependent recovery and the receptor-mediated inhibition. These findings suggested that relevant enzymes may be involved in these phenomena.

Exogenous application of PIP_2 decreased the ATP sensitivity of C-terminal-truncated Kir6.2 (Kir6.2ΔC26), which was functionally expressed on the plasma membrane by itself (8, 26). The neutralization of positively charged amino acid residue R177 or R176 in Kir6.2 reduced the level of functional expression and delayed the time course of the activation by PIP_2 (6, 7),

suggesting that the target of PIP_2 was Kir6.2. In the present study, M_1-receptor stimulation attenuated the effect of pinacidil (Fig. 5). Because the target of pinacidil is SUR (2), this finding supports the finding that PIP_2 modulated the function of SUR1 as well as Kir6.2 (27).

The receptor-mediated inhibition of the K_{ATP} current appears contradictory to the previous report in cat atrial myocytes; using the nystatin-perforated patch method, M_1-receptor stimulation activated the whole-cell K_{ATP} current (28). This discrepancy might arise from different experimental conditions; in the nystatin-perforated patch experiment, intracellular metabolism and Ca^{2+} transient are kept intact. Intracellular ATP consumption may increase by means of the extrusion of intracellular Ca^{2+} and the phosphorylation by PKC during the activation of PI signal transduction pathway. In contrast, the pipette solution used in the present study contained 10 mM BAPTA and 5 mM MgATP. The change of ATP concentration and the activation of Ca^{2+}-dependent PKC may be minimized under this condition. Therefore, we hypothesized that the effects of PIP_2 depletion were observed separately from those of the change of intracellular ATP level and PKC activation. When PKC was directly applied to the patch membrane isolated from the cardiac myocytes, the open probability of the K_{ATP} channel was decreased, and the stoichiometry of the dose-inhibition curve for ATP was modified without changing IC_{50} (29). In the whole-cell patch experiment, PKC activation by phorbol 12,13-didecanoate induced the K_{ATP} current (30). However, in the present study, we have demonstrated that independent of phosphorylation by PKC, the change in PIP_2 level could drastically regulate the K_{ATP} channel. The balance between these factors may determine the properties of the K_{ATP} channel in the native tissues during the stimulation of PLC-linked receptors. PIP_2 has been reported to regulate the activity of the inward-rectifier K^+ channel, GIRK channel, and Na^+-Ca^{2+} exchanger (31). Therefore, the receptor-mediated regulation of the PIP_2 pool may play an important role in the control of cellular function through the modulation of ion channels and transporters.

We thank Prof. A. Noma, Prof. M. Hirata, Dr. F. Yanaga, Dr. Y. Kono, and Dr. T.M. Ishii for discussion. We also thank Prof. S. Seino for SUR2A cDNA, Prof. K. Fukuda for M_1 receptor cDNA, and Dr. K. Moriyoshi for GFP (S65A) cDNA. Technical support from Mr. M. Fukao and Ms. K. Tsuji is highly appreciated. This study was supported by a Grant-in-Aid for Scientific Research (to M.T.) and a Grant-in-Aid on the Priority Area of ATP-binding protein (to M.H.) from the Ministry of Education, Science, Sports and Culture of Japan.

1. Ashcroft, S. J. & Ashcroft, F. M. (1990) *Cell. Signalling* **2,** 197–214.
2. Inagaki, N. & Seino, S. (1998) *Jpn. J. Phyisol.* **48,** 397–412.
3. Yokoshiki, H., Sunagawa, M., Seki, T. & Sperelakis, N. (1998) *Am. J. Physiol.* **274,** C25–C37.
4. Takano, M. & Ashcroft, F. M. (1994) *Pflügers Arch.* **428,** 194–196.
5. Hilgemann, D. W. & Ball, R. (1996) *Science* **273,** 956–956.
6. Fan, Z. & Makielski, J. C. (1997) *J. Biol. Chem.* **272,** 5388–5395.
7. Shyng, S. L. & Nichols, C. G. (1998) *Science* **282,** 1138–1141.
8. Baukrowitz, T., Schulte, U., Oliver, D., Herlitze, S., Krauter, T., Tucker, S. J., Ruppersberg, J. P. & Fakler, B. (1998) *Science* **282,** 1141–1144.
9. Anderson, R. A., Boronenkov, I. V., Doughman, S. D., Kunz, J. & Loijens, J. (1999) *J. Biol. Chem.* **274,** 9907–9910.
10. Majerus, P. W., Kisseleva, M. V. & Norris, F. A. (1999) *J. Biol. Chem.* **274,** 10669–10672.
11. Jenkinson, S., Nahorski, S. R. & Challiss, R. A. (1994) *Mol. Pharmacol.* **46,** 1138–1148.
12. Willars, G. B., Nahorski, S. R. & Challiss, R. A. (1998) *J. Biol. Chem.* **273,** 5037–5046.
13. Inagaki, N., Gonoi, N., Clement, J. P., IV, Namba, N., Inazawa, J., Gonzalez, G., Aguilar-Bryan, L., Seino, S. & Bryan, J. (1995) *Science* **270,** 1166–1170.
14. Sakura, H., Ämmälä, C., Smith, P. A., Gribble, F. M. & Ashcroft, F. M. (1995) *FEBS Lett.* **377,** 338–344.
15. Inagaki, N., Gonoi, N., Clement, J. P., IV, Wang, C.-Z., Aguilar-Bryan, L., Bryan, J. & Seino, S. (1996) *Neuron* **16,** 1011–1017.
16. Ogata, N & Tetebayashi, H. (1991) *J. Neurosci. Methods* **39,** 175–183.
17. Ishii, T., Hashimoto, T. & Ohmori, H. (1996) *J. Physiol.* **493,** 371–384.
18. Fan, Z., Nakayama, K. & Hiraoka, M. (1990) *J. Physiol.* **430,** 273–295.
19. Hilal-Dandan, R., Urasawa, K. & Brunton, L. L. (1992) *J. Biol. Chem.* **267,** 10620–10624.
20. Larsson, O., Barker, C. J., Sjöholm, A., Carlqvist, H., Michell, R. H., Bertorello, A., Nilsson, T., Honkanen, R. E., Mayr, G. W., Zwiller, J. & Berggren, P.-O. (1997) *Science* **278,** 471–474.
21. Nakanishi, S., Catt, K. J. & Balla, T. (1995) *Proc. Natl. Acad. Sci. USA* **92,** 5317–5321.
22. Meyers, R. & Cantley, L. C. (1997) *J. Biol. Chem.* **272,** 4348–4290.
23. Cross, M. J., Stewart, A., Hodgkin, M. N., Kerr, D. J. & Wakelam, J. O. (1995) *J. Biol. Chem.* **270,** 25352–25355.
24. Nakanishi, S., Yano, H. & Matsuda, Y. (1995) *Cell. Signalling* **7,** 545–557.
25. Xie, L.-H., Takano, M., Kakei, M., Okamura, M. & Noma, A. (1999) *J. Physiol.* **514,** 655–665.
26. Tucker, S. J., Gribble, F. M., Zhao, C., Trapp, S. & Ashcroft, F. M. (1997) *Nature (London)* **387,** 179–183.
27. Koster, J. C., Sha, Q. & Nichols, C. G. (1999) *J. Gen. Physiol.* **114,** 203–214.
28. Lipsius, S. L. & Wang, Y. G. (1997) *J. Mol. Cell. Cardiol.* **29,** 907–914.
29. Light, P. E., Sabir, A. A., Allen, B. G., Walsh, M. P. & French, R. J. (1996) *Circ. Res.* **79,** 399–406.
30. Hu, K., Duan, D., Li, G.-R. & Nattel, S. (1996) *Circ. Res.* **78,** 492–498.
31. Huang, C. L., Feng, S. & Hilgemann, D. W. (1998) *Nature (London)* **391,** 803–806.